Talbert et al Figure S1.

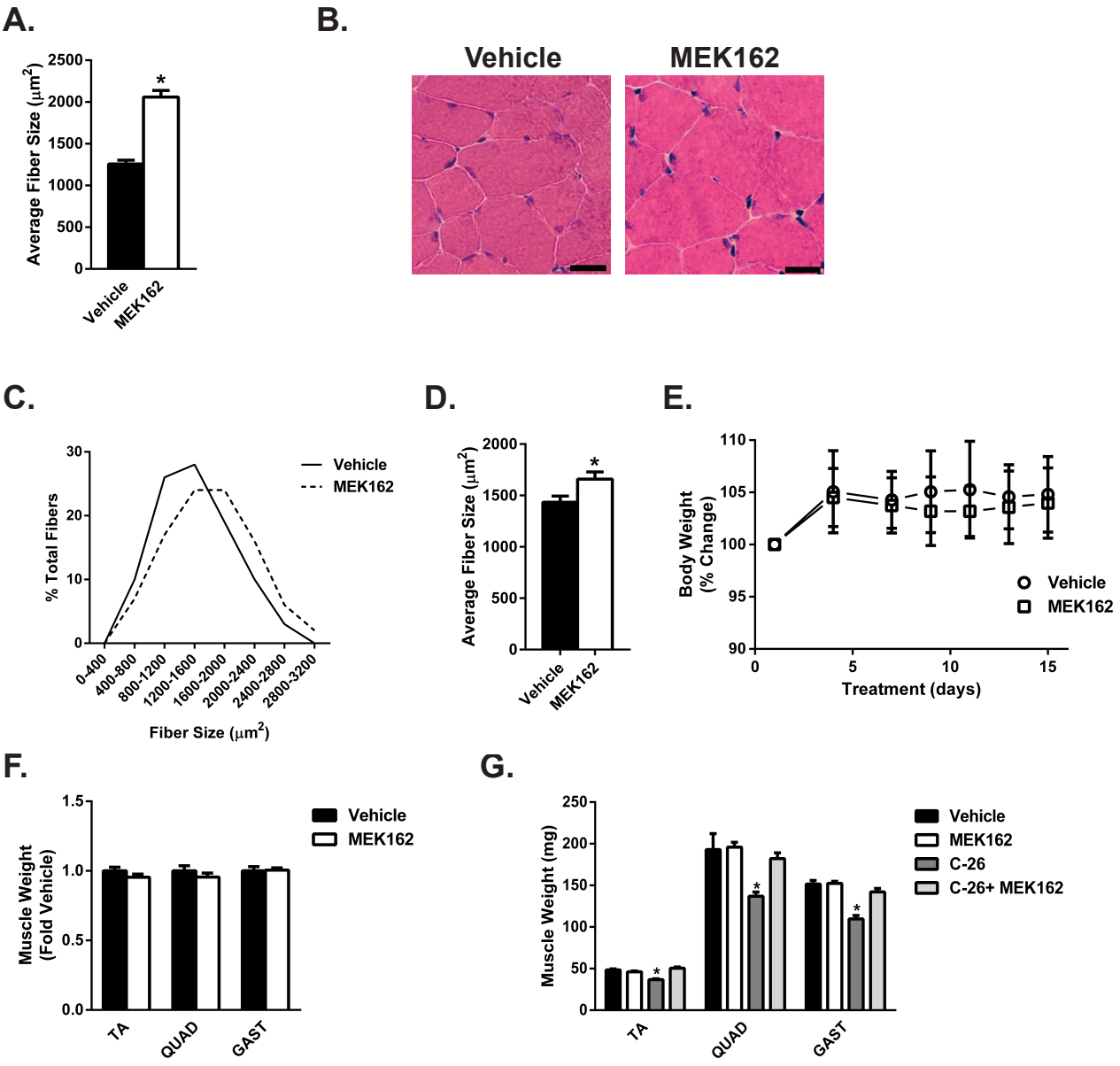

Supplementary Figure 1. MEK162 treatment prevents cancer-induced weight loss and muscle wasting. (A) Mice bearing C-26 tumors and treated with MEK162 have significantly larger average GAST muscle fiber sizes compared to vehicle-treated mice (A log transformation was performed to eliminate heteroscedasticity). **(B)** Representative cross-sections demonstrating muscle fiber size from vehicle and MEK162-treated mice bearing LLC tumors. Scale bar = 20 μm **(C)** Treatment of mice bearing LLC tumors with MEK162 results in a right shift of GAST muscle fiber cross-sectional areas. **(D)** Mice bearing LLC tumors treated with MEK162 have significantly larger average GAST muscle fiber sizes compared to vehicle-treated mice. **(E)** Treatment of control, non-tumor-bearing CD2F1 mice with MEK162 does not alter mouse body weight. **(F)** Treatment of control, non-tumor-bearing CD2F1 mice with MEK162 does not increase muscle mass. **(G)** Treatment of C-26 bearing mice with MEK162 results in muscle masses that are similar to those of control mice without tumors. Data are presented as mean ± standard error of the mean (SEM).n=5-7/group, * = $p<0.05$ compared to vehicle-treated mice.

Talbert et al Figure S2.

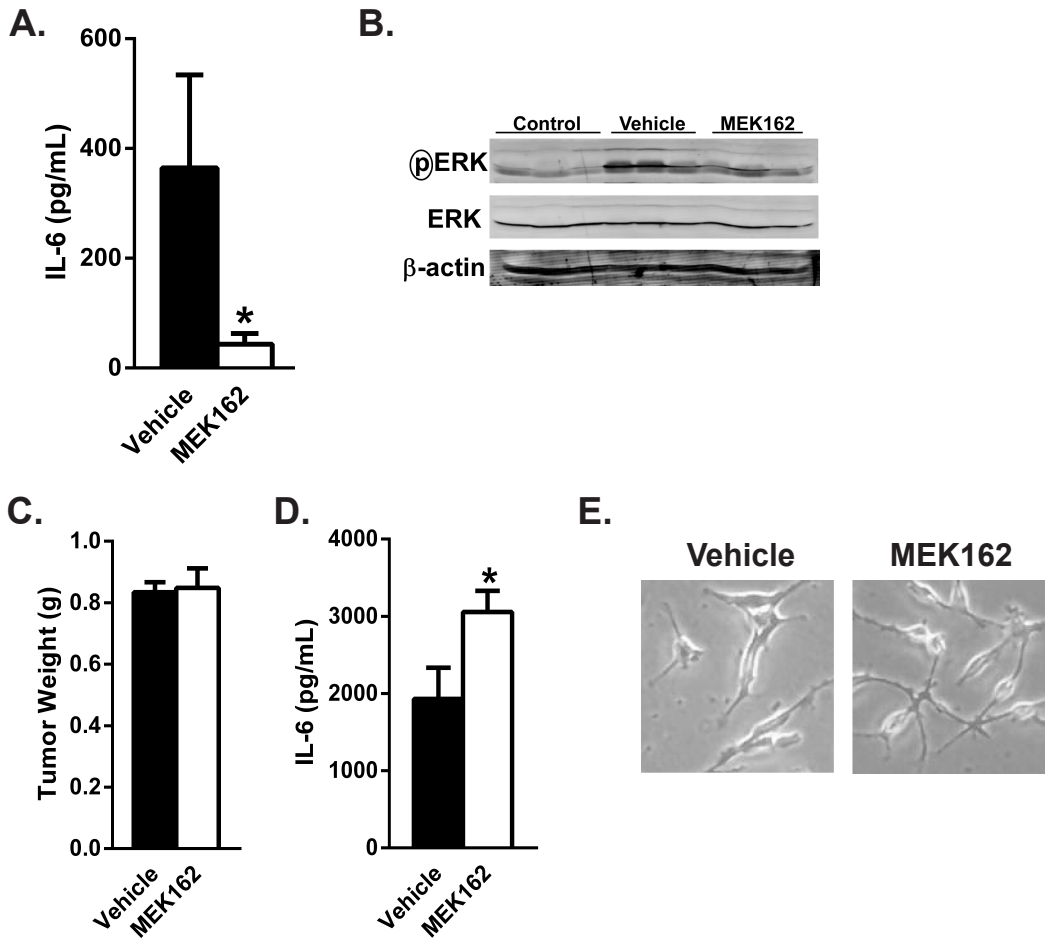

Supplementary Figure 2. Development of a MEK162 resistant C-26 tumor cell line. **(A)** MEK162 treatment reduces serum IL-6 levels of C-26 tumor-bearing mice. **(B)** C-26 induced-cachexia activates ERK signaling in QUAD muscle compared to control, non-tumor-bearing mice, and treatment with MEK162 decreases ERK activation in muscle. **(C)** MEK162 treatment has no impact on C-26R tumor weight at the 19 day time point. **(D)** MEK162 treatment leads to an increase in serum IL-6 in C-26R tumor-bearing mice, supporting that C-26R cells are resistant to MEK162 in vivo. **(E)** C-26R cells appear morphologically different that C-26 cells, with C-26 cells exhibiting a rounded phenotype, while C-26R cells are elongated and display cellular projections. Data are presented as mean ± standard error of the mean (SEM). n=5-11/group, * = $p<0.05$ compared to vehicle-treated mice.

Talbert et al Figure S3.

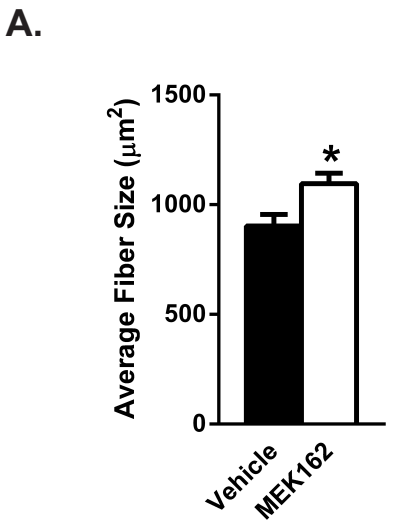

Supplementary Figure 3. MEK162 prevents cancer-induced weight loss and muscle wasting in part via a tumor extrinsic mechanism. (A) C-26R tumor-bearing mice have increased average GAST fiber cross-sectional area. Data are presented as mean ± standard error of the mean (SEM). n= 5/group, * = $p<0.05$ compared to vehicle-treated mice.

Talbert et al Figure S4.

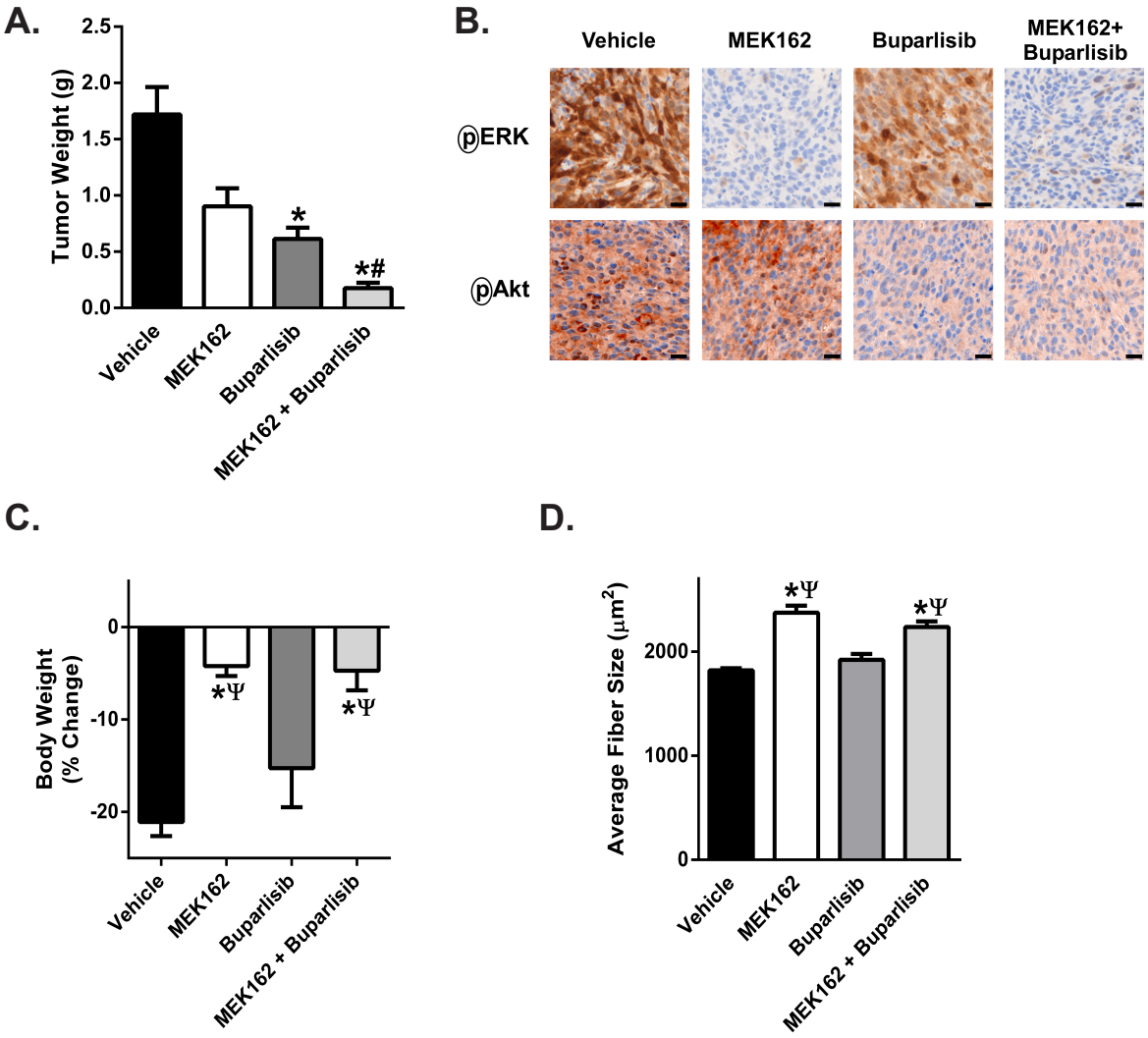

Supplementary Figure 4. MEK162 prevents cancer-induced weight loss and muscle wasting when used in combination with buparlisib. (A) Buparlisib was sufficient to decrease tumor weight, with MEK162+ buparlisib further decreasing tumor weight (A log transformation was performed to eliminate heteroscedasticity). **(B)** MEK162 and buparlisib have on-target effects, and on-target effects are maintained when MEK162 and buparlisib are dosed in combination. **(C)** Vehicle-treated mice lost more body mass than mice treated with MEK162 alone or in combination with buparlisib. **(D)** Treatment of C-26 tumor-bearing mice with MEK162 either alone or in combination with buparlisib results in increased average GAST muscle fiber cross-sectional area (CSA) compared to vehicle-treated mice (A log transformation was performed to eliminate heteroscedasticity). Data are presented as mean ± standard error of the mean (SEM). n=5-6/group. * = $p<0.05$ compared to vehicle-treated mice. # = $p<0.05$ versus both single agent MEK162 and single agent buparlisib. Ψ = $p<0.05$ versus single agent buparlisib.

Talbert et al Figure S5.

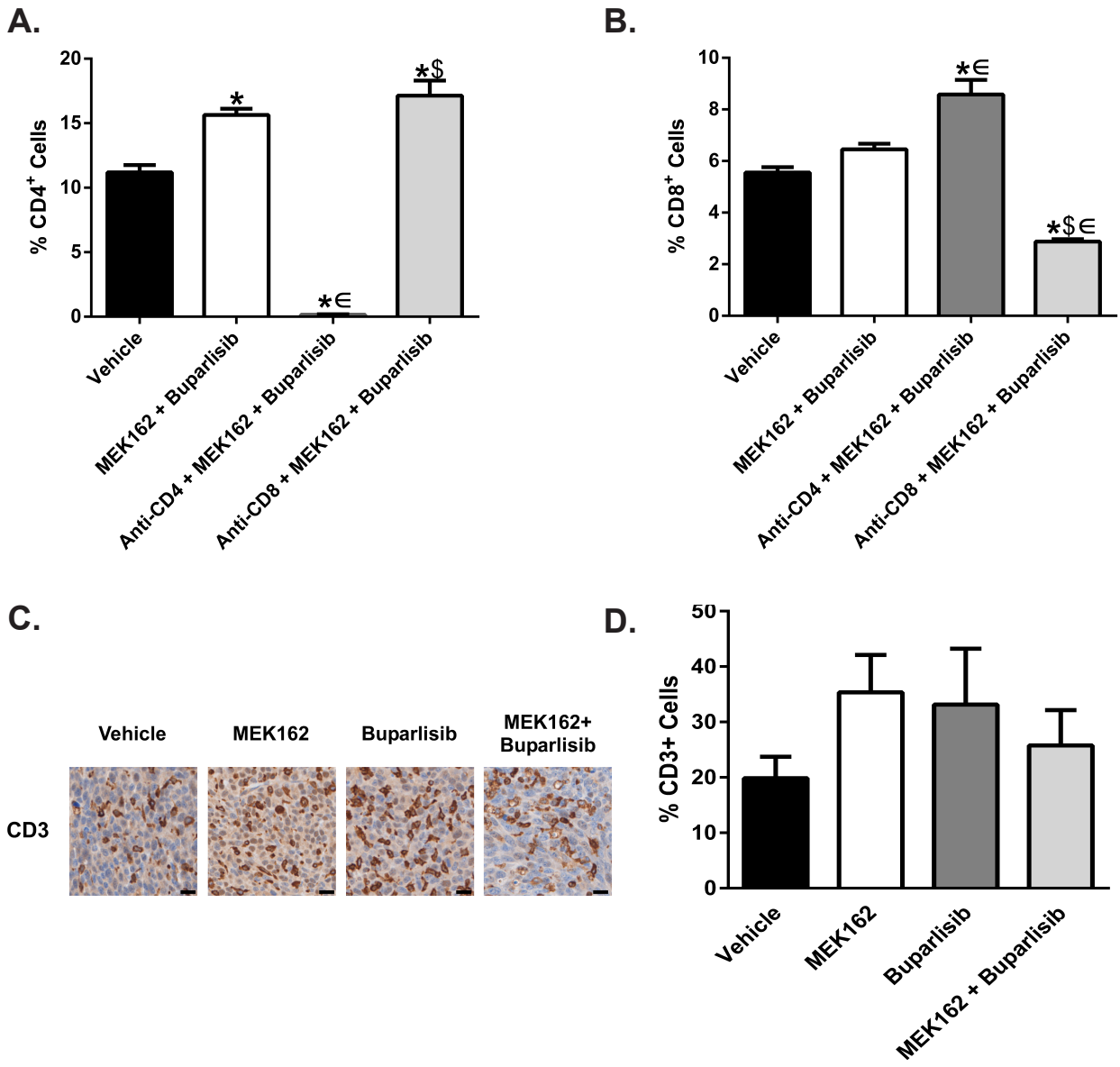

Supplementary Figure 5. MEK162 and buparlisib modulate immune biomarkers.
(A) CD4+ cell depletion was effective, as the number of splenic CD4+ T cells is reduced in mice treated with anti-CD4 antibody. **(B)** CD8+ cell depletion was effective, as the number of CD8+ T cells was decreased in mice treated with anti-CD8 antibody. **(C)** Representative images of CD3+ cells in C-26 tumors. **(D)** Infiltration of CD3+ cells in tumors does not differ between groups. Data are presented as mean ± standard error of the mean (SEM). n=5-6/group. * = $p<0.05$ compared to vehicle-treated mice. € = $p<0.05$ versus MEK162 + buparlisib. $ = $p<0.05$ versus Anti-CD8 + MEK162 + buparlisib.

Gene	Primer Pairs	Size (bp)
Atrogin-1	5’ - AGATTCGCAAGCGTTTGATC - 3’ 5’ - GGGAAAGTGAGACGGAGCAG - 3’	204
MuRF1	5’ - TGGCGATTGTCACAAAGTGG - 3’ 5’ - CCCTCTCTAGGCCACCGAGT - 3’	100
Mul1	5’ - AGGGCATTCTTTCAGAAGCA - 3’ 5’ - GGGGTGGAACTTCTCGTACA - 3’	329
Musa1	5’ - CAGAGGATTGGGACGGGACG - 3’ 5’ - GTGAGTGCTGCTGTACCTCTT - 3’	167
Atg5	5’ - ATCAGACCACGACGGAGCGG - 3’ 5’ - GGCGACTGCGGAAGGACAGA - 3’	116
Bnip3	5’ - CAGAGCGGGGAGGAGAAC - 3’ 5’ - GAGGCTGGAACGCTGCTC - 3’	80
GAPDH	5’ - AGCCTCGTCCCGTAGACAAAA - 3’ 5’ - GCCTTGACTGTGCCGTTGATT - 3’	199

Supplementary Table 1. Primer sequences used for real-time RT-PCR.